

1 **Seasonal variation of mercury concentration of ancient olive**
2 **groves of Lebanon.**

3
4 Nagham Tabaja^{1,2,3}, David Amouroux⁴, Lamis Chalak², François Fourel⁵, Emmanuel Tessier⁴,
5 Ihab Jomaa⁶, Milad El Riachy⁷, Ilham Bentaleb¹

6
7 ¹ ISEM, Univ Montpellier, CNRS, IRD, Montpellier, France

8 ² Faculty of Agronomy, Plant Production Department, The Lebanese University, Dekwaneh, Lebanon

9 ³ Plateforme de Recherche et d'Analyses en Sciences de l'Environnement (PRASE), Ecole Doctorale de Sciences et
10 Technologie, Université Libanaise, Hadath, Liban

11 ⁴ Université de Pau et des Pays de l'Adour, E2S/UPPA, CNRS, Institut des Sciences Analytiques et de Physico-Chimie
12 pour l'Environnement et les Matériaux (IPREM), PAU, France

13 ⁵ UMR CNRS 5023 LEHNA, Université Claude Bernard Lyon 1, Villeurbanne, France

14 ⁶ Department of Irrigation and Agrometeorology, Lebanese Agricultural Research Institute (LARI), P.O. box 287,
15 Zahle, Lebanon

16 ⁷ Department of Olive and Olive Oil, Lebanese Agricultural Research Institute (LARI), P.O. box 287, Zahle, Lebanon

17
18 *Correspondence to:* Ilham Bentaleb (Email: ilham.bentaleb@umontpellier.fr, Tel: +33(0) 6 38 61 57 69)

19
20

21 **Abstract.** This study investigates the seasonality of the mercury (Hg) concentration of olive trees foliage, an iconic
22 tree of the Mediterranean basin. Hg concentrations of foliage, stems, soil surface, and litter were analyzed on monthly
23 basis in ancient olive trees growing in two groves in Lebanon, Bchaaleh and Kawkaba (1300 and 672 m.a.s.l.
24 respectively). A significantly lower concentration was registered in stems (~7-9 ng/g) with respect to foliage (~35-48
25 ng/g) in both sites with the highest foliage Hg concentration in late winter-early spring and the lowest in summer. It
26 is noteworthy that olive fruits also have low Hg concentration (~7-11 ng/g). The soil has the highest Hg content (~62-
27 129 ng/g) likely inherited through the cumulated litter biomass (~ 63-76 ng/g). A good covariation observed between
28 our foliage Hg time-series analysis and those of atmospheric Hg concentrations available for southern Italy in the
29 western Mediterranean basin confirms that mercury pollution can be studied through olive trees. Spring sampling is
30 recommended if the objective is to assess the tree's susceptibility to Hg uptake. Our study draws an adequate baseline
31 for Eastern Mediterranean and the region with similar climatic inventories on Hg vegetation uptake. In addition to
32 being a baseline to new studies on olive trees in the Mediterranean to reconstruct regional Hg pollution concentrations
33 in the past and present.

34 **Keywords:** Eastern Mediterranean, ancient groves, *Olea europaea* L., mercury pollution, plant tissues, soil and litter

35 **Introduction**

36
37 Mercury (Hg) is among the most widely distributed potentially toxic metals polluting the Earth (Briffa et al. 2020). It
38 is found as all heavy metals naturally on the Earth's crust reservoir and in the atmosphere through the natural long-
39 term Hg biogeochemical cycle (i.e., volcanic activities, geological weathering). This metal is easily modified into
40 several oxidation states and it can also be spread through many ecosystems (Boening 2000). The natural Hg cycle has
41 been modified due to anthropogenic activities (i.e., mining, smelting, soil erosion due to deforestation, gold extraction,
42 agriculture-fertilizers, manure) (Patra and Sharma 2000). Among natural and anthropogenic Hg emissions, inorganic
43 elemental Hg (Hg(0)) is the most dominant chemical form. It is primarily transferred through the atmosphere by air
44 mass movement and can undergo long-range transport. Because of its high volatility and susceptibility to oxidation,
45 elemental Hg(0) is the predominant form of Hg in the atmosphere that can be accumulated into foliage. This highly
46 diffusive Hg can easily pass biological barriers (i.e. cell membranes, foliage, skin). Mercury has three oxidation states,
47 namely, Hg(0) (elemental mercury), Hg(I) (mercurous), or Hg(II) (mercuric), although Hg(I) mercurous form is not
48 stable under typical environmental conditions and, therefore, is rarely observed. It is likely that the Hg(II) high binding
49 affinities bind covalently with organic groups (Du and Fang, 1983; Clarkson and Magos 2006; Pleijel et al., 2021).
50 The exchange of Hg between the soil and plants is not stable and is variable dependent (e.g. cation-exchange capacity,
51 soil pH, soil aeration, and plant species) (Patra and Sharma 2000). Forests are known to act as a sink of atmospheric
52 Hg. Plant foliage takes up of Hg deposited on leaf surfaces through the stomata (i.e. Leaf gas exchange) and leaf
53 cuticles (Hanson et al. 1995; Jiskra et al. 2018; Li et al. 2017; Lodenius et al. 2003; Maillard et al. 2016; Rea et al.
54 2002; Yanai et al. 2020) where it accumulates with minimal mobility and small portions released back into the
55 atmosphere or transferred to other plant organs (Cavallini et al. 1999; Hanson et al. 1995; Li et al. 2017; Lodenius et
56 al. 2003; Schwesig and Krebs 2003). All together these authors contributed to highlight the dynamic role of the foliar
57 surfaces in terrestrial forest landscapes acting as a source or sink dependent on the magnitude of current Hg

58 concentrations. Hanson et al. (1995) suggested a species-specific compensation concentrations (or compensation
59 points) for Hg deposition.

60 Hg is redistributed to the forest floor through litter and throughfall and hence passes to the soil (Rea et al. 1996). The
61 Hg input through the litter is greater than the input from that of the wet deposition (Wang et al., 2016). Litter has been
62 estimated to constitute 30 to 60 % of the Hg atmospheric deposition in Europe and North America forests (Rea et al.
63 1996; Blackwell and Driscoll 2015; Zhou et al. 2018). According to Wright et al., (2016) the litter Hg is the dominant
64 pathway in forests where it contributes 53 to 90 % of the dry deposition to the forest. In terrestrial ecosystem, soils
65 have the highest Hg reservoir (Obrist et al., 2018; O'Connor et al., 2019) followed by trees (Yang et al., 2018). This
66 Hg is provided by natural geological sources and natural events such as forest fires, volcanic eruptions (Ermolin et al.
67 2018; Obrist et al. 2018; O'Connor et al. 2019) and anthropogenic sources (UNEP, 2019). Though variable from year
68 to year, Hg emission to the atmosphere from biomass burning is considered as an important driver of the global Hg
69 biogeochemical cycle (Friedli et al., 2009; De Simone et al., 2015; McLagan et al., 2021; Dastoor et al., 2022). Soil
70 can also release Hg to the atmosphere (Luo et al., 2016; Assad, 2017; Yang et al., 2018; Schneider et al., 2019; Gworek
71 et al., 2020; Pleijel et al., 2021) and also behave as a source of Hg to the plants. Hg of the soil is taken up by the
72 roots along with the water, it is translocated to other parts (ie. Stems, Leaves) of the plant using the xylem sap (Bishop
73 et al., 1998; Li et al., 2017). This pathway ~~have~~ has been described on several plant species in Hg contaminated sites
74 (Assad et al. 2017). Trees are hence considered as important drivers of Hg exchange between the atmosphere and the
75 soil (Yang et al. 2018). The recent studies on Hg uptake by vegetation have highlighted the importance of the role of
76 different parameters as vapor pressure deficit, soil water content, climatic conditions, date of sampling, leaf mass area,
77 tree functional groups, stomatal conductance, affecting potentially the root uptake of Hg dissolved in soil water and
78 the absorption rate via stomata and eventually the Hg leaf content (Rea et al., 2002; Obrist et al., 2011; Blackwell &
79 Driscoll, 2015; Yang et al., 2018; Wohlgemuth et al., 2021). In polluted sites the soil is the main source of Hg to the
80 vegetation while away from those sites the atmosphere is the most important source (Naharro et al., 2018). The Hg
81 source in foliage varies with respect to the amount of contamination (Hanson et al., 1995).

82 The studies of the Hg cycle in forest ecosystems show that gaseous elemental Hg(0) is the main source taken up by
83 plants (Bishop et al. 2020; Zhou et al. 2021). Analysis of long term atmospheric Hg(0) and CO₂ concentrations are
84 very informative to understand the role of the vegetation in the global Hg cycle (Jiskra et al., 2018). Emission reduction
85 measures adopted in Europe and North America since the 70s are corroborated by Hg dendrochemistry analysis
86 showing a declining Hg concentration trend from the older to newer tree rings. Indeed, tree ring Hg
87 (dendrochronology) is a powerful archiving tool for atmospheric Hg(0). After Hg(0) oxidation inside the leaves, Hg(II)
88 bind to organic compounds and then is transported to the bole wood via the phloem (Beauford et al., 1977; Lindberg
89 et al., 1979). This is corroborated by the recent study of McLagan et al., (2022) showing the benefit of the stable Hg
90 isotope analysis on dendrochemistry. Several studies have evidenced seasonal variations of the atmospheric Hg(0)
91 contents (ie. in temperate Northern Hemisphere by Jiskra et al., 2018; in Western Mediterranean Basin in South Italy
92 (Martino et al. 2022) with high values in winter and low values in summer. Interestingly, Jiskra et al., (2018) show
93 also a significant positive correlation between the monthly Hg(0) and CO₂ concentrations. They highlighted a one-
94 month offset in Hg(0) summer time minima happening in September in comparison to the CO₂ minima value occurring

95 in August, this trend is not observed in winter time. The uptake of Hg(0) by the vegetation continues during CO₂
96 respiration periods during the fall and night when the ecosystem exchange of CO₂ turns from being a sink to becoming
97 a source (Wofsy et al., 1993; Jiskra et al., 2018).

98 The total gaseous Hg (TGM) in the Mediterranean atmosphere is similar to Northern Europe (1.3 to 2.4 ng m⁻³) (Kotnik
99 et al. 2014). In the case of a semi-closed sea such as the Mediterranean basin with warm summers, high sea-water
100 evaporation, solar radiations and Hg anthropogenic sources, the Mediterranean Sea acts as a net source of Hg to the
101 global atmosphere (Kotnik et al. 2014) making the Mediterranean an air-pollution emission area (Baayoun et al. 2019;
102 Borjac et al. 2019).

103 The olive tree (*Olea europaea* L.) is one of the most distinctive Mediterranean agro-ecosystems tree species (Besnard
104 et al., 2013), and is adapted to drought (Sghaier et al. 2019). Considered to be among the oldest trees in the
105 Mediterranean basin, centennial olive trees are still growing in many countries along both the eastern and western
106 shore, surviving numerous stresses and are of considerable historical, cultural and ecological importance (Terral et al.
107 2004). The olive tree still remains a key component of agriculture today and will be into the future. Therefore, genetic
108 characterization of olive varieties and genetic resources (Khadari et al., 2019; Galatali et al., 2021), description based
109 on morphological characters and phenology of growth stages of olive trees (Sanz-Cortés et al., 2002), experimentation
110 through field irrigation and/or more rarely through drought stress treatments (Alcaras et al., 2016) have been conducted
111 to avoid genetic erosion, optimize the water use for irrigation and hence improve orchard management, and solely to
112 better understand the biodiversity. Only few studies have focused on the response of the olive tree to Hg pollution in
113 its natural Mediterranean environment (Higuera et al., 2012; Higuera et al., 2016; Guarino et al., 2021; Labdaoui et
114 al., 2021).

115 Lebanon, a small country at the Eastern Mediterranean, is facing important anthropogenic pressure within a changing
116 environment (Gérard and Nehmé 2020). The air quality in Lebanon all over the country is noted to be moderately
117 unsafe with an annual mean concentration of 31 µg/m³ of PM_{2.5} (Particulate Matter) which is above the maximum
118 recommended value (10 µg/m³) (Lebanon: Air Pollution IAMAT 2020). Adding to that, soil samples collected from
119 different areas in southern Lebanon showed values of Hg concentration ranging between 160-6480 ng/g showing a
120 high contamination levels (Borjac et al. 2020) as indicated by World reference Senesil et al., 1999; Kabata-Pendias &
121 Pendias, 2000. The main contributors of the air pollution include cement industries, mineral and chemical factories,
122 vehicles emissions, food processing and oil refining. Ancient olive groves are found across different agroclimatic
123 areas at different altitudinal belts, still producing olives and oil for consumption with these various pollution pressures.
124 In this study two sites, known for their century-old olive groves and located at two different altitudes in Lebanon,
125 were selected to assess the Hg contents. In these remote areas, no direct sources of mercury contamination are reported
126 and hence we expect very low Hg concentrations. However, due to atmospheric transport of Hg, dry or wet deposition
127 of Hg can be expected in remote areas (Grigal, 2003). The main objectives of this study are to examine and compare
128 Hg levels in foliage, stems, fruits, litter and soil measured in each of these two olive groves, which we monitored
129 monthly for 18 months. The second objective is to analyze the relative importance of Hg uptake by the soil and foliage
130 in comparison with the atmospheric Hg. Since the distribution of Hg pollution is by nature geographically widespread,
131 and given the extent of Hg pollution in the Mediterranean and the transfer of pollution by wind and the Mediterranean

132 Sea, long-distance contamination occurs over large areas. This study may draw an adequate baseline for Eastern
133 Mediterranean and region of similar climates inventories on Hg vegetation uptake and new studies on olive trees in
134 the Mediterranean to reconstruct regional Hg pollution concentrations in the past and present.

135 **2. Materials and methods**

136
137 Two monumental olive groves were chosen in the context of their historical and agricultural importance,
138 since these two sites are considered to contain olive trees more than 1400 years old and are still productive.

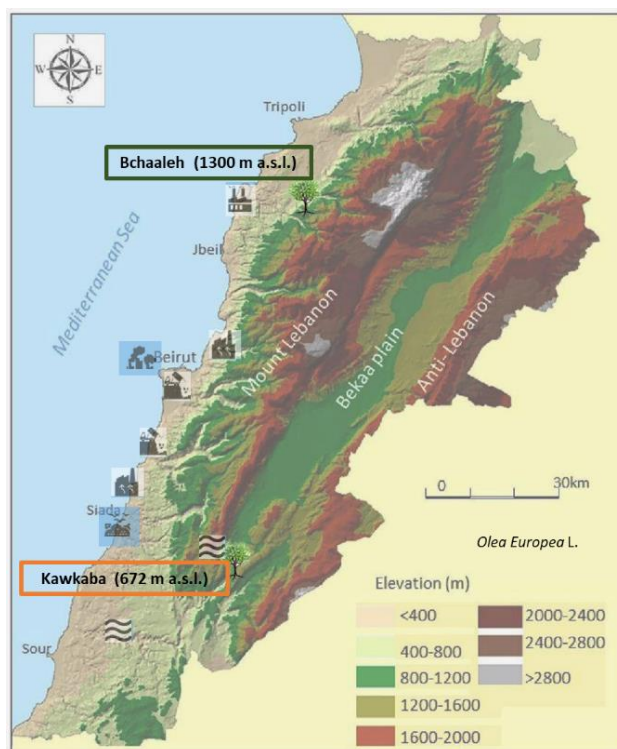
139 **2.1. Geographic setting and environmental context**

140 141 **2.1.1. Bchaaleh site - North Lebanon**

142
143 This grove is situated in Batroun district (Latitude 34°12'06'' N, Longitude 35°49'23'' E, Altitude 1300 m.a.s.l.)
144 (Figure 1). Olive trees are growing rainfed in a sandy loam texture soil of grain size analysis of sand, silt and clay
145 percentages are 52.8 %, 38.7 % and 10.7 % respectively. Soil pH is 7.07 ± 0.26 with organic matter and calcium
146 carbonate contents are 1.7 % and 38.3 % respectively (Yazbeck et al. 2018). In this study, soil profiles of carbon and
147 nitrogen contents were analyzed. Organic carbon contents decreased with soil depth from about 4 % at 0-1 cm (Soil
148 surface) to 2.7 % at 30-60 cm. The total nitrogen is about 0.3 % at 1cm depth and 0.2 % at 30-60 cm depth. The olive
149 trees are located on two terraces. The first terrace is at 1.5 meter above the road level while the second is at the road
150 level. They are maintained by the municipality for the last four decades as an endowment property. Precipitation
151 average ranges between 229 and 392 mm in winter and between zero and less than 2 mm/season in summer, while
152 average temperature is between 4 and 8 °C in winter and between 20 and 23 °C in summer and average relative
153 humidity of 63% (data extracted from LARI climatic data) (Table S1, Figure S1).

154 The village is at about 36 km from Chekka town located at a lower altitude (0-200 m.a.s.l.) nearby the sea (Figure 1),
155 and which is classified as a source of air pollution (EJOLT 2017). Chekka is the site of an important national cement
156 factory responsible of carbon dioxide, sulfur dioxide, nitrous oxides, carbon monoxide and particulate material
157 emissions causing respiratory and health issues (Kobrossi et al. 2002) and water pollution (Nassif et al. 2016). At 28
158 km from Bchaaleh, the small commercial port of Selaata (0-37 m.a.s.l.) emits many pollutants (ie. Phosphogypsum,
159 heavy metals, radionuclides) expanding via water and air pathways (Petrlik et al. 2013; Yammine et al. 2010). To our
160 knowledge no direct Hg pollution is reported at Chekka and Selaata sites. However a dissolved gaseous Hg from
161 natural and human activities is saturated in the upper Eastern Mediterranean Sea, Gårdfeldt et al., (2003) have
162 evidenced that Mediterranean Sea is a source of airborne elemental Hg.

163



164
 165 **Figure 1.** Site locations of the two selected focus areas (modified after Shared Water Resources of Lebanon, Nova
 166 Science Publishers 2017).
 167

168 **2.1.2. Kawkaba site - South Lebanon**
 169

170 The second grove is located in the village of Kawkaba, South Lebanon (Latitude 33°23'856'' N, Longitude
 171 35°38'588'' E, Altitude 672 m.a.s.l. (Figure 1). Kawkaba soil is characterized as clay loam soil of pH 7.5 ± 0.5 . Soil
 172 organic material and calcium carbonate average are 1.7 % and 59.0 % respectively (Al-Zubaidi et al., 2008) and grain
 173 size analysis of sand, silt and clay percentages are 6 %, 28 % and 66 % respectively. The analysis of organic carbon
 174 and nitrogen at the 0-1 cm and at 0-30 cm decrease from about 9.0 % to 2.2 % and from 0.9 % to 0.3 % for the carbon
 175 and nitrogen respectively. Average precipitation ranges between 215 and 374 mm in winter and drop to almost zero
 176 mm in summer, while average temperature is between 7 and 11 °C in winter and between 21 and 27 °C in summer
 177 and relative humidity of 61% (data extracted from LARI climatic data) (Table S1, Figure S1).

178 The village has to its east the Hasbani river, originated from the north-western slopes of Mount Hermon in Hasbaya
 179 (36 km away from Kawkaba and located at 750 m.a.s.l.) (Badr et al. 2014; Jurdi et al. 2002). On the other hand, the
 180 Litani River (170 km long and located at 800 to 1000 m.a.s.l) (Figure 1) rising in the south of the Bekaa valley is
 181 about 29 km away from Kawkaba (Abou Habib et al. 2015, Khatib et al. 2018). These two rivers are polluted and for
 182 these reasons they are not used for irrigating crops in Kawkaba and surrounding areas while the olive trees are growing
 183 rainfed as per indicated by the municipality of Kawkaba. Here as well, we did not find indication of direct Hg pollution.
 184 Climatic data in both Bchaaleh and Kawkaba were collected from meteorological station and manual rain gauge
 185 installed in the villages by LARI (Lebanese Agricultural Research Institute). CO₂ data used in this study are from
 186 NOAA Global Monitoring Laboratory (https://gml.noaa.gov/webdata/ccgg/trends/co2/co2_trend_gl.txt).

187 **2.2. Field sampling**

188
189 For the Hg concentration analysis, four olive trees (3-5 m in diameter and an average height of 4-6 m) were sampled
190 in each of the two groves from February 2019 to September 2020. Within Bchaaleh two trees were selected from the
191 upper terrace (BCO1-Bchaaleh-Tree 1, BCO4-Bchaaleh-Tree 4) and two other trees were sampled from a lower
192 terrace located 1.5 m below the upper one (BCO9-Bchaaleh-Tree 9, BCO12-Bchaaleh-Tree 12) (Figure S2). In
193 Kawkaba, four trees were selected and sampled (KWO1-Kawkaba-Tree 1, KWO2-Kawkaba-Tree 2, KWO3-
194 Kawkaba- Tree 3, KWO4-Kawkaba-Tree 4). For each olive tree, both sun exposed and shaded foliage and stems
195 (terminal portions of 20 cm) with no evidence of pathogens were randomly taken and merged from the upper, middle,
196 and lower canopy position of the olive trees on a monthly basis using a manual pruner. The phenological growth stages
197 of olive trees described by Sanz-Cortés et al.,(2002) in Spain suggest leaf development from March to November.
198 Hence it should be mentioned that the Hg concentration measured on monthly collected foliage represents an average
199 of Hg accumulated in young foliage (year N of collection where N is equal to 2019 and 2020) and older foliage (N-1
200 year and N-2 years). Fruits were collected in April 2019. Litter and soil surface were separately collected on the whole
201 top surface area of the olive groves and stored in different paper bags once every four months. In parallel, soil sampling
202 was performed using a bucket auger to a maximum depth of 60 cm. In both sites Bchaaleh and Kawkaba, the soil
203 showed uniform color and texture. Soil cores were fractioned in soil surface (0-1 cm), 0 to 30 cm depth and from 30
204 to 60 cm depth in order to study the effect and accumulation of Hg concentration on the different depth layers. To
205 avoid contamination, gloves were worn while collecting samples, and the equipment was rinsed with methanol
206 between every sample. A set of 453 samples were collected and stored in paper bags until further preparation for the
207 Hg analysis.

208

209 **2.3. Sample preparation for Hg analysis**

210
211 Collected foliage and stems were rinsed with distilled water and then dried for 48 hours in an oven at a temperature
212 of 50°C at maximum (Demers et al., 2013; Li et al., 2017; Pleijel et al., 2021). This procedure likely eliminate any
213 Hg(0) present in the samples. The dried foliage, stems, litter and olive fruits samples were grinded using an electrical
214 stainless grinding machine with no heating system for 5-10 minutes, while soil samples were prepared with a manual
215 natural agate grinder. All samples were later sieved using an inox stainless-steel 125-micron sieve mesh to collect
216 homogeneous powders for analysis. A total of 150 mg for foliage and soil (50 mg/analysis), and 300 mg of litter and
217 stems (100 mg/analysis) were considered in triplicates for analysis of Hg concentrations.

218

219 **2.4. Analytical method**

220
221 For the Hg elemental analysis, a total of 453 powder samples from foliage, stem, grain, litter and soil were analyzed
222 using an advanced Hg analyzer AMA 254 (Altec) as described elsewhere (Barre et al. 2018; Duval et al. 2020). A
223 known amount of sample (50-100 mg) is weight in a nickel boat, using a 10⁻⁶ g precision balance. The sample aliquot
224 is first dried at 120°C for 60s and subsequently pyrolyzed at 750°C for 150s, under oxygen flow. The resulting gaseous

225 Hg produced during the sample decomposition is amalgamated on a gold trap and then released to an Atomic
226 Absorption spectrometer after a thermal desorption step at 950°C. The AMA 254 instrument was calibrated through
227 several external matrix-matched calibration procedures using the following certified reference materials: IAEA-456
228 sediment (77 ± 5 ng Hg/g), NIST-1575A pine needles ($39,9 \pm 0,7$ ng Hg/g) and IAEA336 (200 ± 40 ng Hg/g). The
229 QA/QC evaluation of the analytical procedure was completed with a continuous monitoring of the blank's values
230 (Nickel boat Hg background noise), every 15 analyzed samples. The precision of the measurements was assessed
231 through replicated analyses (n=2) of 13 % of the total amount of samples (n=453). Average relative standard deviations
232 of 5 % and 2.5 % are thus associated to the reported Hg concentrations for the 2019 and 2020 samples batches,
233 respectively. The absolute detection limit (ADL) of the analytical technique (AMA 254) was estimated at 0.04 ng Hg.
234 As a consequence, the method detection limit (MDL) for samples analyzed were 0.7 ng Hg/g for soil, litter and foliage
235 and 0.4 ng Hg/g for stem and wood. These MDL were much lower than the measured Hg concentration in the various
236 samples.

237 Subsamples of soil were used for carbon and nitrogen elemental contents (%) analysis. A 2 mg (acid washed soil and
238 bulk soil) of powders were weighed into tin capsules and measured by dry combustion using a Pyrocube Elemental
239 Analyser (EA, Elementar GmbH).

240

241 **2.5. Statistical analysis**

242

243 For the statistical analysis we used the R 4.1.0 program. Our data are not normally distributed, so for the effect of
244 tissue type on Hg concentration, Wilcoxon test was used with the tissue type (foliage and stems) as the main effect.
245 Pearson correlation analysis was used to examine the inter-individual correlation of Hg concentration between the
246 trees. Correlation between Hg concentration of soil surface, litter and foliage was studied using a correlation test. For
247 the seasonal effect (Winter: Mid December till Mid-March, Spring: Mid-March till Mid-June, Summer: Mid-June till
248 Mid-September, Autumn: Mid-September till Mid-December) on Hg concentration, Wilcoxon test was used
249 considering the unequal data available for the different seasons. Finally, the effect of climatic factors (Temperature,
250 precipitation, pCO₂) on Hg accumulation was examined using a Wilcoxon test.

251

252 **3. Results**

253

254 **3.1. Hg concentrations in plant tissues, litter and soil at Bchaaleh and Kawkaba groves**

255

256 Hg concentrations measured in the different sampled materials (plant tissues, litter and soil) varied generally according
257 to both tree tissues and groves agroclimatic conditions (Table 1). Hg values in the foliage varied significantly between
258 the two groves (p-value= $1.581 \cdot 10^{-6}$), where the highest concentration was recorded in Bchaaleh (48.1 ± 10.6 ng/g)
259 vs. (35 ± 12.4 ng/g) in Kawkaba. Soil surface also recorded a difference in Hg concentration between Bchaaleh and
260 Kawkaba, with 61.9 ± 20.0 ng/g in Bchaaleh and 128.5 ± 9.4 ng/g in Kawkaba. Soil 0-30 cm samples taken from
261 Bchaaleh and Kawkaba groves, values ranged between 31.8 ± 4.7 ng/g and 70.2 ± 23.4 ng/g respectively. In soil 30-
262 60 cm Hg concentrations recorded 19.5 ± 6.73 ng/g at Bchaaleh. No significant differences were recorded for litter

263 and stems Hg concentrations (p-value= 0.0915 and p-value=0.2215 respectively) between the groves, with litter values
 264 of 62.9 ± 17.8 at Bchaaleh and 75.7 ± 20.3 ng/g at Kawkaba vs. stem values of 7.9 ± 2.8 ng/g at Bchaaleh and $9.0 \pm$
 265 4.7 ng/g at Kawkaba. Positive correlations were observed between soil and litter in Bchaaleh ($r=0.60$) and Kawkaba
 266 ($r=0.95$) though statistically insignificant (p-value= 0.40 and 0.13 respectively).

267 The comparison between Bchaaleh and Kawkaba soil surface Hg contents showed significant difference between the
 268 two groves (p-value=0.04746). We observe the same significant difference when comparing the soil horizon of 0-30
 269 cm of both groves. In descending order of Hg concentrations and considering the different sites, plant tissue, soil and
 270 litter samples, the Hg concentrations could be ranked in Bchaaleh, soil surface > litter> foliage > soil 0-30 cm > soil
 271 30-60 cm > stems > fruits; and in Kawkaba, soil surface > litter > soil 0-30 > foliage > soil 30-60 > stems > fruits
 272 (Table 1).

273
 274 **Table 1.** Overall mean values of Hg concentration (ng/g) of the different studied material in both Bchaaleh and
 275 Kawkaba olive groves
 276

Sample material	Bchaaleh (BC)			Kawkaba (KW)		
	Average (ng/g)	SD	N	Average (ng/g)	SD	N
Foliage	48.1	10.6	66	35.0	12.4	67
Stems	7.9	2.8	66	9.0	4.7	67
Litter	62.9	17.8	7	75.7	20.3	6
Soil Surface	61.9	20.0	8	128.5	9.4	6
Soil 0-30cm	31.8	4.7	6	70.2	23.4	5
Soil 30-60cm	19.5	6.7	5	28.0		1
Fruits	7.0	3.5	3	11.0		1

277
 278 **3.2. Seasonal variation of Hg concentration in plant tissues, litter and soil**
 279

280 Hg concentrations recorded between February 2019 and September 2020 (Table 2) reflected a significant seasonal
 281 variation in both sites (p-value< 2.2×10^{-16})

282 In Bchaaleh grove, foliage registered its highest Hg concentration during winter and spring with 61.8 ± 7.6 ng/g and
 283 55.1 ± 12.5 ng/g respectively, and its lowest Hg amount during summer and autumn with 41.5 ± 12.7 ng/g and $44.4 \pm$
 284 6.2 ng/g, respectively. A seasonal effect on foliage and stems was registered (p-value< 2.2×10^{-16} ; Figure 2a,c). The
 285 stems and soil 0-30cm highest values was registered in autumn. Significant differences were found in foliage Hg
 286 values between summer and winter (p-value=0.00020), and autumn and winter (p-value= 0.00014). Similarly, stems
 287 Hg values varied significantly between spring and winter (p-value=0.030), autumn and winter (p-value=0.047). Litter
 288 highest Hg content occur in summer in Bchaaleh olive groves (79.3 ± 26.5 ng/g) and the lowest in winter (48.6 ± 13.3
 289 ng/g) (p-value = 0.2286). Highest Hg contents in the soil surface of Bchaaleh is recorded in summer (84.5 ± 21.2
 290 ng/g).

291 In Kawkaba, the highest Hg concentrations for foliage and stems were registered in spring with 51.8 ± 4.5 ng/g, 11.7
 292 ± 6.7 ng/g respectively (Table 2, Figure 2b,d). Significant differences were found in foliage Hg values between

293 summer and winter (p-value=0.013), autumn and winter (p-value= 0.00067), autumn and spring (p-value=1.589*10⁻
 294 ⁰⁵), spring and winter (p-value= 9.383*10⁻⁰⁵) and spring and summer (p-value=2.327*10⁻⁰⁶). Similarly, stem Hg values
 295 varied significantly between spring and winter (p-value=0.006), spring and summer (p-value=0.0036) and autumn and
 296 spring (p-value=0.011). There is no seasonal variation between the litter different seasons for Bchaaleh nor for
 297 Kawkaba. Bchaaleh and Kawkaba groves soil surface, 0-30 cm and 30-60cm Hg values varied significantly between
 298 seasons, (p-value < 0.05). A seasonal variation is observed in both olive groves especially in the foliage.

299
 300 **Table 2.** Seasonal mean Hg concentration (ng/g) and standard deviations of the different studied material in both
 301 Bchaaleh and Kawkaba olive groves. Grey color indicated the highest Hg concentration values among the different
 302 material during the different seasons.
 303

Hg (ng/g)												
Bchaaleh	Spring	SD	N	Summer	SD	N	Autumn	SD	N	Winter	SD	N
Foliage	55.1	12.5	16	41.5	12.7	24	44.4	6.2	12	61.8	7.6	18
Stems	7.8	3.8	16	7.61	3.9	24	8.3	2.7	12	6.4	2.9	18
Litter	79.3	26.5	3	64.7	4	4	55.5	3.54	2	48.6	13.3	3
Soil Surface	58.3	13	3	84.5	21.2	4	50		1	50.6	23.5	3
0-30cm	33.6	6.2	2	32.2	4.3	2	34.5	7.79	2	27	0.7	3
30-60cm	23.1	9.1	2	20.7	10.32	2	19.6	9.05	2	11		1
Kawkaba	Spring	SD	N	Summer	SD	N	Autumn	SD	N	Winter	SD	N
Foliage	51.8	4.5	16	28	7.2	24	28.5	7.2	16	33.9	5.6	18
Stems	11.7	6.7	16	6.5	1.4	24	7.7	2.1	16	6.9	1.6	18
Litter	90.1	29.3	2	67	24	2	70	1.4	2			
Soil Surface	132	8.5	2	118	4.2	2	135.6	2.2	2			
0-30cm	57.9	11.2	2	65.8		1	84.8	36.4	2			
30-60cm	28		1									

304
 305

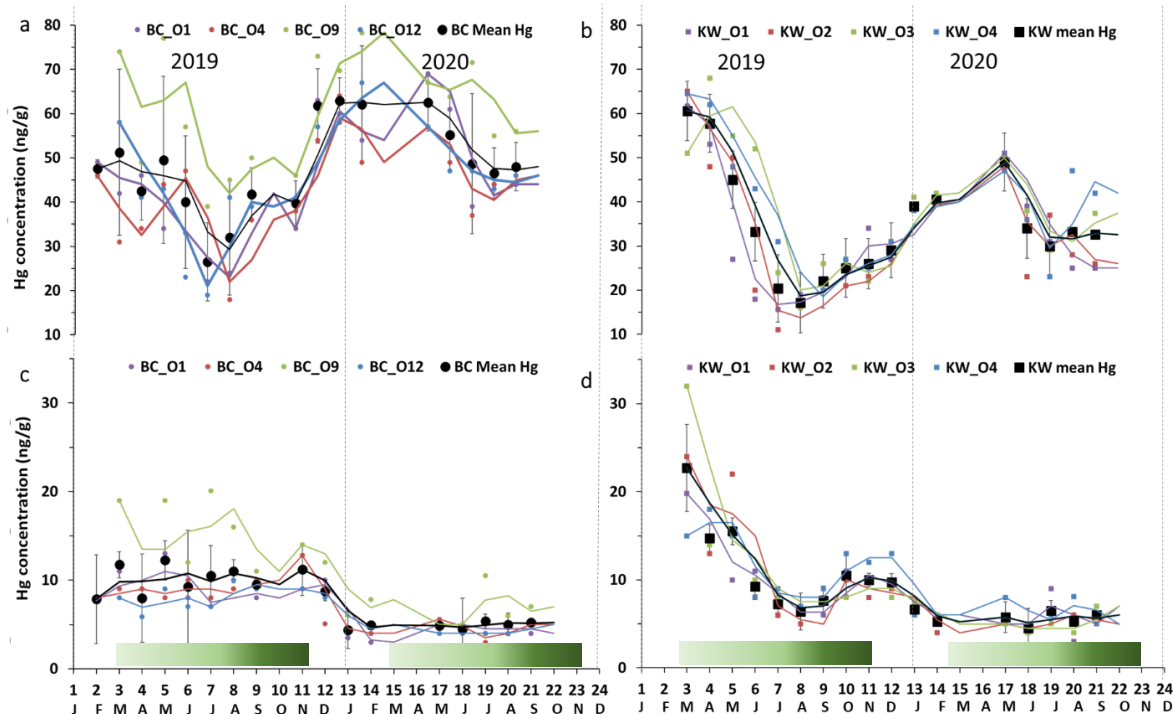


Figure 2. Seasonal variations of foliage Hg concentration in (a) Bchaaleh (BC) and (b) Kawkaba (KW) olive groves and stems Hg concentration in (c) Bchaaleh and (d) Kawkaba olive groves. Shaded green horizontal bars represent the leaf development of olive trees during the growing season of cultivars in Spain according to the BBCH scale (Sanz-Cortès et al., 2002).

3.3. Inter-individual variability between trees for each site

In the upper terrace of Bchaaleh grove, the foliage average Hg concentration of BCO4 and BCO1 varied between 42.4 ± 11.5 ng/g and 44.6 ± 13.3 ng/g respectively showing no significant difference (p -value = 0.8225). In the lower terrace of the same site, foliage average Hg concentrations of trees BCO12 and BCO9 were found to vary from 45.6 ± 12.7 ng/g to 60.7 ± 12.7 ng/g respectively (Figure 2a) exhibiting a significant difference (p -value=0.0059). Tree BCO9 is significantly different to each of the three trees (p -value< 0.0059) while BCO1, BCO4 and BCO12 have very similar Hg contents (p -value= 0.46).

In the upper terrace of Bchaaleh grove, the stems average Hg concentration of BCO4 and BCO1 varied between 7.0 ± 2.8 ng/g and 7.1 ± 2.9 ng/g respectively showing no significant difference (p -value= 0.94). In the lower terrace, stems average Hg concentrations of BCO12 and BCO9 are 6.4 ± 2.2 ng/g and 11.2 ± 5.2 ng/g respectively showing a significant difference (p -value= 0.0054; Figure 2c). For BCO1 and BCO12 there was no significance difference (p -value= 0.5725), the same goes for BCO4 and BCO12 (p -value= 0.523).

The average concentration per tree in foliage and stems were 32.4 ± 12.2 ng/g and 8.5 ± 4.0 ng/g respectively for KWO1, 32.8 ± 14.7 ng/g and 8.9 ± 6.0 ng/g for KWO2, 37.6 ± 14.0 ng/g and 9.3 ± 6.7 ng/g for KWO3 and 37.7 ± 13.6 ng/g and 9.6 ± 4.0 ng/g for KWO4 (Figure 2b,d). In Kawkaba grove, comparison of the foliage Hg concentration between the four studied trees shows no significant difference ($0.22 < p$ -value<1), neither for the stems ($0.21 < p$ -value<0.96).

331 **3.4. Hg concentration and agro-climatic effect**

332
333 At first glance, seasonal variations of the Hg concentrations of the foliage of both sites suggest a covariation with
334 climatic parameters (Precipitation amounts, Relative Humidity and Temperature) (Figure SI) and atmospheric pCO₂.
335 Foliage Hg content increased with higher precipitation and lower temperature (Autumn and Winter) while during the
336 warmer and dryer seasons (May to mid-October), the Hg concentration of foliage decreased (Figure SI). However, the
337 Wilcoxon test for a non-normal distribution shows no significant correlation between Hg concentration of foliage and
338 precipitation (p-value= 0.95). While temperature, relative humidity and atmospheric CO₂ (pCO₂) shows a significant
339 correlation (p-value = $2.2e^{-16}$). For the stems, Hg concentration also showed no significant correlation with
340 precipitation (p-value=0.1147), and a significant correlation with temperature, relative humidity and pCO₂ (p-value=
341 $2.2e^{-16}$).

342 **4. Discussion**

343 344 **4.1. Hg concentration in plant tissues, soil and litter in the studied groves**

345
346 In both groves our values showed a higher Hg concentration in the olive foliage (Bchaaleh average of 48.1 ± 10.6
347 ng/g; Kawkaba average of 35.0 ± 12.4 ng/g), than that of the stems (Bchaaleh average of 7.9 ± 2.8 ng/g; Kawkaba
348 average of 9.0 ± 4.7 ng/g) and that of olive fruits (7 ± 3.5 ng/g at Bchaaleh, n=3 and 11 ng/g in Kawkaba, n=1). Our
349 data corroborates previous studies (Bargagli 1995; Higuera et al. 2016) showing that olive foliage has the highest Hg
350 concentration of plant tissues. Our values are lower than 200 ng/g considered as Hg pollution threshold (Kabata-
351 Pendias & Pendias, 2000) and implying no pollution effect for both Bchaaleh and Kawkaba groves (Table S2; Figure
352 S3a,b). This suggests that our sites are good remote bioindicators of the uptake of Hg through the plant, although more
353 prolonged time range study is needed. However, in an overview of vegetation uptake of mercury and impacts on global
354 cycling, Zhou et al., (2021) suggested lower values for unpolluted sites (litterfall 43 ng/g > foliage 20 ng/g and branch
355 12 ng/g). Knowing that our sites correspond to unpolluted areas of Lebanon, the lower values of Zhou et al., (2021)
356 obtained from an ensemble of various species (trees and grasses) and not specifically on olive trees, we considered
357 that the threshold value of 200 ng/g (Kabata-Pendias and Pendias 2000) is more adapted to our comparison.

358 As described in several studies, Hg in foliage originates predominantly from the atmospheric gaseous Hg(0) through
359 stomatal uptake (Ericksen et al., 2003; Lindberg et al., 1979; Zhou et al., 2021). Adding to that, the atmospheric Hg
360 uptake in foliage exceeds Hg stomatal re-emission (Pleijel et al., 2021; Zhou et al., 2021). Inside the leaves the oxidized
361 Hg(II) has high affinities to bind covalently with organic groups (Du & Fang, 1983; Clarkson & Magos, 2006; Pleijel
362 et al., 2021). The Hg can be translocated by phloem transport to the stems and eventually into roots and potential
363 release into soils may also be contributing to Hg accumulation in soils (Giesler et al., 2017; Schaefer et al., 2020).

364 The soil surface and litter registered the highest Hg concentration (62 to 129 ng/g) among all samples (foliage, stems,
365 fruit) in both groves (Table 1) suggesting that the soil is the main Hg reservoir through the Hg throughfall and litter
366 inputs (Tomiyasu et al., 2005). Our findings are in agreement with studies on evergreen forest ecosystems reporting
367 that soil can hold more than 60 % of Hg input to the forest floor (Wang et al. 2016). Our soil surface sites values (61.9
368 ± 20.0 ng/g in Bchaaleh and 128.5 ± 9.4 ng/g in Kawkaba) show higher Hg concentration in Kawkaba compared to

369 the general background level of Hg as defined by uncontaminated soil world reference mean Hg contents (20 to 100
370 ng/g; Kabata-Pendias and Pendias 2000; Senesil et al. 1999; Gworek et al. 2020). However, both sites have
371 significantly lower values compared to known industrial and mining contaminated sites (> 1000 ng/g ;). Nevertheless,
372 studies conducted in different sites show a wide range of natural background Hg levels (ie. topsoils in Europe, India,
373 Brazil, Norwegian Arctic, New Zealand have values of 40, 50, 80, 110, 230 ng/g respectively) (Gworek et al. 2020)
374 making it difficult to set a specific Hg threshold value for uncontaminated soil (Table S2; Figure S3c). Due to the
375 differences registered in different countries and sites of sampled soil, this indicates a link with chemical and
376 mineralogical soil properties (ie. pH, humic acid, soil grain size distribution, organic matter type and clay percentage)
377 affecting Hg in soil and its transport (Richardson et al., 2013; Chen et al., 2016; O'Connor et al., 2019). Nitrogen can
378 also be a factor affecting the Hg content in soil depending on its characteristics. Nitrogen increase can change the
379 equilibrium of soil solution and the morphology of roots, causing a possible increase in Hg availability in soil and
380 increases the Hg uptake by the plant (Alloway, 1995; Barber, 1995; Carrasco-Gil et al., 2012). The increase in Hg
381 availability in the soil is due to the organic Nitrogen that provides a high absorption capacity, retaining the atmospheric
382 Hg deposition (Obrist et al., 2009). Nitrogen supply prevents oxidative stress in roots, but also can improve root
383 development and increase the uptake of Hg from the soil (Carrasco-Gil et al. 2012). Hence, we suggest that lower
384 values in Bchaaleh soils are likely explained by the low clay, organic carbon and nitrogen contents (10.7 %, 4 % and
385 0.3 % in soil surface respectively). While Kawkaba higher Hg soil contents can be explained by the higher clay
386 proportion (66 %) and organic carbon and nitrogen contents (9 % and 0.92 %). On such clay loam soils and rich
387 organic matter, Hg binding is facilitated explaining higher content (O'Connor et al. 2019).

388 The litter showed higher Hg concentration than that in foliage in both Bchaaleh (62.9 ± 17.8 ng/g) and Kawkaba (75.7
389 ± 20.3 ng/g) (Table 1). This has been also described by Rea et al., (1996) and Zhou et al., (2021) in uncontaminated
390 and contaminated sites where litterfall Hg contents were systematically higher than the foliage Hg contents. The
391 bacterial and chemical decomposition of the litter decrease significantly the amount of C compared to the Hg that
392 conversely may continue to increase due to the continued absorption of Hg from precipitation and throughfall (Obrist
393 et al., 2011; Pokharel & Obrist, 2011; Zhou et al., 2021). Another possible explanation is that the leaves shed as litter
394 are likely to mostly be the oldest leaves which have accumulated Hg during the longest period of time and thus have
395 higher Hg concentrations than the remaining foliage have on average since they consist of both younger and older
396 foliage (Rea et al. 1996; Pleijel et al. 2021).

397

398 **4.2. Seasonal foliage Hg content versus seasonal atmospheric Hg and CO₂**

399

400 The late winter-early spring registered the highest Hg concentration for foliage in both groves, while summer and
401 early fall to a less extent recorded the lowest concentrations. This seasonal change is explained by the seasonal tree
402 physiology variations such as the Hg accumulation in leaves after stomatal uptake (Pleijel et al., 2021; Wohlgemuth
403 et al., 2021). We can suggest that during winter-early spring, water is available and photosynthetic activity is not
404 limited, hence both CO₂ and Hg diffuse through opened stomata inside the foliage. As shown on figure 2, Hg in foliage
405 is low in summer-fall and hence act as a sink of Hg. A clear seasonal pattern of Hg concentration in foliage is evident,
406 despite being based on three generation of olive leaves (1-3 years old), with youngest leaves known to have low

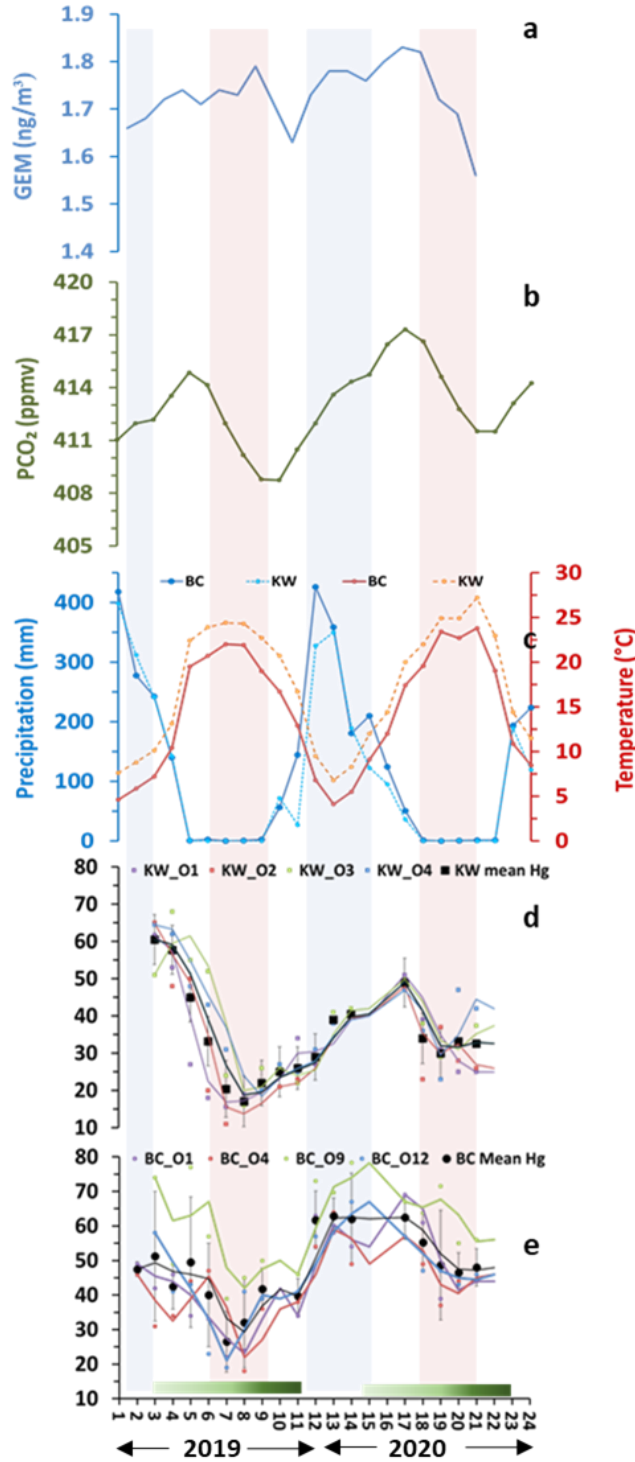
407 concentrations (Pleijel et al., 2021), the seasonal signal is still very remarkable. Therefore, one can speculate that the
408 mercury levels would have been higher if we had avoided the recently formed foliage during spring and early summer.
409 This may also explain the large difference in Hg levels between litter and foliage.

410 Evergreen olive foliage at our sites show a decrease in Hg contents from end of March to late August, with minimum
411 values centered in August suggesting a decline of the plant Hg uptake likely explained by the reduction of the stomatal
412 conductance (Lindberg et al., 2007; Pleijel et al., 2021). This minimal photosynthetic activity occurs during the driest
413 season (0 mm precipitation) and hottest temperatures (above 25°C) at our sites. For the period 2018-2020, Martino et
414 al. (2022) showed an atmospheric GEM depletion when NDVI values increased (normalized difference vegetation
415 index). This can explain the lower foliage Hg content in 2019 compared to 2020 at our study sites in Lebanon. This
416 was also collaborating Jiskra et al., (2018) for the Northern Hemisphere site. Since no data of atmospheric mercury in
417 Lebanon or surrounding countries are available we used the atmospheric Hg time series data of Martino et al. (2022)
418 (Figure 3a). We observed opposite trends between foliage Hg concentration and air Hg (negative covariation in 2019
419 and positive covariation in 2020) (Figure a,d,e).

420 Alternatively other studies reported a positive correlation between atmospheric Hg and crops (Niu et al. 2011) as
421 observed in our study between the Hg_{foliage} and the atmospheric Hg in 2020 (Figure 3a,d,e). This suggest the hypothesis
422 where our groves seasonally exposed to high atmospheric Hg, accumulate Hg in their foliage (Lindberg et al. 2007;
423 Pleijel et al. 2021). According to Hanson et al. (1995), a compensation point for Hg uptake by plant foliage can be
424 considered but no information to our knowledge is available for the specific case of the olive trees. The tight link
425 between foliage Hg uptake and stomatal conductance seasonal variations can be also deduced from the analysis of the
426 partial pressure of the pCO_{2atm} seasonal variation (Obrist, 2007; Jiskra et al., 2018; Obrist et al., 2018; Pleijel et al.,
427 2021) (Figure 3b,d,e). Very good covariation between olive foliage Hg and pCO_{2atm} are shown for Bchaaleh and
428 Kawkaba despite a notable offset of one month at Kawkaba to two months at Bchaaleh can be deduced (Figure S4).

429 Taking into account our calculated time lags, we obtained significant correlations between our foliage Hg content and
430 pCO_{2atm} of 0.718 and 0.704 in Bchaaleh and Kawkaba respectively. Interestingly a one month time-lag between
431 atmospheric Hg and pCO_{2atm} is also reported by Jiskra et al. (2018) for most northern hemisphere sites. The offset of
432 one to two months between maxima of Bchaaleh and Kawkaba foliage Hg (March/April) and pCO_{2atm} (May) suggests
433 that the minimum of Hg in the foliage occur during the decreasing phase of the pCO_{2atm} when the global northern
434 hemisphere tend to become a net sink of CO₂. When minimum values of pCO_{2atm} are reached at the end of the dry
435 summer (Figure 3b), concomitant to minimum atmospheric Hg (Figure 3a), end of the drought and increase of
436 precipitation (Figure 3c), Bchaleh and Kawkaba olive trees show a recovery in the Hg uptake rates. The photosynthetic
437 activity and the stomatal conductance related to the climatic parameters (temperature, precipitation, humidity, pCO₂)
438 as shown by Ozturk et al. (2021) and the atmospheric Hg explain our foliage Hg seasonal cycle. At a regional scale,
439 our sites show different time lags between Bchaaleh and Kawkaba that we cannot explain fully except their altitudinal
440 differences, which can suggest that Bchaaleh grove benefits of less drought in summer.

441



442
443
444
445
446
447
448

Figure 3. Seasonal variations of (a) atmospheric Hg(0) (Martino et al. 2022), (b) pCO₂ (NOAA Global Monitoring Laboratory), (c) precipitations and temperature of Bchaaleh and Kawkaba respectively and (d) and (e) foliage Hg concentration in Bchaaleh and Kawkaba olive groves respectively. Shaded green horizontal bars represent the leaf development of olive trees during the growing season of cultivars in Spain according to the BBCH scale (Sanz-Cortès et al., 2002). Shaded colored lines correspond to the Winter (Blue) and Summer (Red).

449 **4.3. Hg cycling in the stems, litter and soil system**

450
451 For each site, Hg contents in stems exhibit a narrow range between the different trees except tree BCO9, which had
452 the highest stem values. We speculate that this higher Hg content is the adjunction of chemical products as fertilizer
453 on the plot 549 belonging to a different owner (Figure S2) likely between fall and winter. It was observed by (Zhao &
454 Wang, 2010) that the fertilizer used and its source of phosphorous may affect the Hg content in the product and thus
455 affect the amount of Hg transported into the fertilized soil.

456 At a seasonal scale, the averaged Hg values of soil system show statistically significant differences between the four
457 seasons, while stems show statistically significant differences between winter (lowest values) and spring (p-value=
458 0.030) and winter-autumn (p-value= 0.047) in Bchaaleh grove mostly similar to foliage changes. While litter shows
459 no significant difference between seasons. The same behavior was registered in Kawkaba in litter and soils, while
460 stems showing statistical significance differences between autumn and spring (p-value= 0.011), spring-winter (p-
461 value= 0.006) and spring-summer (p-value= 0.004) (Table 2). Despite the small amount of Hg content in the stems,
462 the statistically significant seasonal changes may suggest that small amount of Hg move from the foliage to the
463 lignified tissues as stems. However, we cannot neglect the Hg transport in xylem sap from the roots to the aboveground
464 plant tissues even if minimal (Yang et al. 2018).

465 We can suggest the following Hg cycling in the system of the olive grove/soil. In winter-early spring the highest
466 concentrations in foliage continuously feed the litter and can explain the following maximal spring Hg content of the
467 litter. The decomposition of the litter organic matter during the wettest conditions likely liberate Hg in the Hg(0) or
468 Hg(II) forms or MeHg either towards the atmosphere or the surface soil (see Table 2) respectively (Gworek et al.,
469 2020). A fraction of the degraded organic matter is transferred through gaseous evaporative processes towards the
470 atmosphere while another fraction of the Hg is leaching towards the deeper soil in addition to dry Hg deposition during
471 dry season (Teixeira et al. 2017). We can also speculate that the small Hg decrease observed in soil 0-30, 30-60 cm
472 during the winter season in Bchaaleh can be due to the minimal absorption of total Hg and MeHg through the roots
473 and xylem sap to the above ground tissues (Johnson and Lindberg 1995).

474 **5. Conclusion**

475
476 This is the first study conducted on monumental olive trees in a-remote site of the MENA region without local
477 contamination and followed at a monthly basis over 18 months. Findings of our study indicate a higher uptake of Hg
478 in the olive foliage compared to stems, fruits items and a remarkable Hg_{Foliage} seasonal variation in both studied groves.
479 Winter and Spring were particularly suitable for Hg accumulation in foliage in both sites. The significant correlation
480 between our Hg_{Foliage} contents and the atmospheric Hg content and pCO_2 , despite the one to two months' time lag,
481 suggests that the main source of Hg_{Foliage} is the atmospheric Hg as observed in different species and studies (conifers
482 and hardwood). Hg is absorbed by the foliage, via the open stomata, driven by the interaction of high vegetal activity,
483 temperature, water availability and the processes that control transpiration, which is likely to be seasonal. Hence
484 physiological and climatic processes explain the seasonal Hg accumulation in foliage. Thus, a more intensive study
485 taking account the phenological dynamics of olive tree foliage must be focused on. Further comparison and studies
486 on the seasonal atmospheric Hg in the eastern Mediterranean basin are necessary to test our hypothesis of the reversed

487 seasonality of Hg in 2019 and positive covariation in 2020 since contrary to the global Northern Hemisphere and
488 western Mediterranean region vegetation, our olive groves act as a sink of Hg and CO₂ when global Northern and
489 western Mediterranean vegetation is emitting. This relationship $Hg_{Foliage} - Hg_{atm} - pCO_{2atm}$ should be further investigated
490 along the season and locally to better understand the observed time lags. Soil surface registered the highest Hg
491 concentration among all studied compartments due to well-known processes of litter and throughfall that incorporate
492 Hg to the soil surface. Moreover, this study highlights significant differences between Hg_{soil} in Bchaaleh and Kawkaba
493 groves due to differences in soil characteristics. In this study we worked on the present time samples in order to have
494 a better understanding of the Hg cycle in the olive tree. Our main contribution in this study is to see how the present-
495 day olive trees records some elements such as Hg to better understand how the Hg in tree rings could be used for the
496 past accumulation records.

497

498 **Data availability**

499 The datasets generated during and/or analyzed during the current study are available from the corresponding author
500 on reasonable request.

501

502 **Author Contributions**

503 The corresponding author **Ilham Bentaleb** is responsible for ensuring that the descriptions are accurate and agreed upon
504 by all authors. Conceptualization and methodology were done and developed by **Ilham Bentaleb** and **Lamis Chalak**.
505 The material collection was performed by **Naghm Tabaja, Ilham Bentaleb, Lamis Chalak, Ihab Jomaa, and Milad**
506 **Riachy**. Sample storage and preparation in Lebanon organized by **Naghm Tabaja**. Material preparation at ISEM by
507 **Naghm Tabaja**, Data collection and analysis were performed by Naghm Tabaja, **Ilham Bentaleb, David Amouroux,**
508 **and Emmanuel Tessier**. The setting of the meteorological stations by **Ihab Jomaa**. Subsamples of soil were analyzed
509 for carbon and nitrogen elemental contents (%) by **François Fourel**. The first draft of the manuscript was written by
510 **Naghm Tabaja, Ilham Bentaleb, Lamis Chalak, David Amouroux, Ihab Jomaa, and Milad Riachy** commented
511 on previous versions of the manuscript. All authors read and approved the final manuscript. Supervision was done by
512 Ilham Bentaleb and Lamis Chalak.

513

514

515 **Competing interests**

516 The authors declare that they have no known competing financial interests or personal relationships that could have
517 appeared to influence the work reported in this paper.

518

519

520 **Acknowledgments**

521 The authors would like to acknowledge the National Council for Scientific Research of Lebanon (CNRS-L) and
522 Montpellier University for granting a doctoral fellowship (CNRS-L/UM) to Naghm Tabaja. The authors would also
523 like to thank the Franco-Lebanese Hubert Curien Partnership (PHC-CEDRE) project 44559PL for the funding
524 provided. Institute of Evolutionary Science of Montpellier (ISEM) at Montpellier University and the Research
525 Platform for Environment and Science- Doctoral School of Science and Technology (PRASE-EDST) at the Lebanese
526 University are also acknowledged for their support of the laboratory work. Credits go to the Lebanese Agriculture
527 Research Institute (LARI) for assuring automated weather stations and manual rain gauges per site. The authors are
528 grateful to the Municipality of Bchaaleh (Mr. Rachid Geagea) and the Municipality of Kawkaba (Ms. Mira Khoury).
529 Acknowledgments are extended to Ms. Amira Yousef at LARI for her kind support and to Mr. Akram Tabaja for
530 helping during fieldwork. We are very grateful to Pleijel Hakan who reviewed this article improving significantly our
531 paper. We deeply acknowledge Andrew Johnston for the English revision.

532 **Funding**

533 This work was supported and funded by Lebanon and Montpellier University (CNRS-L/UM grant), and PHC-
534 CEDRE-project 44559PL

535
536 **References**

- 537
538 Abou Habib, N., Taleb, M., & Khoury, R.: Environmental and social safeguard studies for lake qaraoun pollution
539 prevention project. V1(E4749), 2015.
- 540 Alcaras, L. M. A., Rousseaux, M. C., & Searles, P. S.: Responses of several soil and plant indicators to post-harvest
541 regulated deficit irrigation in olive trees and their potential for irrigation scheduling. *Agricultural Water*
542 *Management*, 171, 10–20. <https://doi.org/10.1016/j.agwat.2016.03.006>, 2016.
- 543 Alloway, B. J.: *Heavy Metals in Soils*. Springer Science & Business Media, 1995.
- 544 Al-Zubaidi, A., Yanni, S., & Bashour, I.: Potassium status in some Lebanese soils. *Lebanese Science Journal*, 9(1),
545 81–97, 2008.
- 546 Assad, M.: Transfert des éléments traces métalliques vers les végétaux: Mécanismes et évaluations des risques dans
547 des environnements exposés à des activités anthropiques. 218, 2017.
- 548 Baayoun, A., Itani, W., El Helou, J., Halabi, L., Medlej, S., El Malki, M., Moukhadder, A., Aboujaoude, L. K.,
549 Kabakian, V., Mounajed, H., Mokalled, T., Shihadeh, A., Lakkis, I., & Saliba, N. A.: Emission inventory of
550 key sources of air pollution in Lebanon. *Atmospheric Environment*, 215, 116871.
551 <https://doi.org/10.1016/j.atmosenv.2019.116871>, 2019.
- 552 Badr, R., Holail, H., & Olama, Z.: Water quality assessment of hasbani river in south lebanon: microbiological and
553 chemical characteristics and their impact on the ecosystem. 3, 16, 2014.
- 554 Barber, S. A.: *Soil Nutrient Bioavailability: A Mechanistic Approach*. John Wiley & Sons, 1995.
- 555 Bargagli, R.: The elemental composition of vegetation and the possible incidence of soil contamination of samples.
556 *Science of The Total Environment*, 176(1–3), 121–128. [https://doi.org/10.1016/0048-9697\(95\)04838-3](https://doi.org/10.1016/0048-9697(95)04838-3),
557 1995.
- 558 Barre, J. P. G., Deletraz, G., Sola-Larrañaga, C., Santamaria, J. M., Bérail, S., Donard, O. F. X., & Amouroux, D.:
559 Multi-element isotopic signature (C, N, Pb, Hg) in epiphytic lichens to discriminate atmospheric
560 contamination as a function of land-use characteristics (Pyrénées-Atlantiques, SW France). *Environmental*
561 *Pollution*, 243, 961–971. <https://doi.org/10.1016/j.envpol.2018.09.003>, 2018.

562 Beauford, W., Barber, J., & Barringer, A. R.: Uptake and Distribution of Mercury within Higher Plants. *Physiologia*
563 *Plantarum*, 39(4), 261–265. <https://doi.org/10.1111/j.1399-3054.1977.tb01880.x>, 1977.

564 Besnard, G., Khadari, B., Navascues, M., Fernandez-Mazuecos, M., Bakkali, A. E., Arrigo, N., Baali-Cherif, D., de
565 Caraffa, V. B.-B., Santoni, S., Vargas, P., & Savolainen, V.: The complex history of the olive tree: From
566 Late Quaternary diversification of Mediterranean lineages to primary domestication in the northern Levant.
567 *Proceedings of the Royal Society B: Biological Sciences*, 280(1756), 20122833–20122833, 2013.

568 Bishop, K. H., Lee, Y.-H., Munthe, J., & Dambrine, E.: Xylem sap as a pathway for total mercury and
569 methylmercury transport from soils to tree canopy in the boreal forest. *Biogeochemistry*, 40, 101–113,
570 1998.

571 Bishop, K., Shanley, J. B., Riscassi, A., de Wit, H. A., Eklöf, K., Meng, B., Mitchell, C., Osterwalder, S., Schuster,
572 P. F., Webster, J., & Zhu, W.: Recent advances in understanding and measurement of mercury in the
573 environment: Terrestrial Hg cycling. *Science of The Total Environment*, 721, 137647.
574 <https://doi.org/10.1016/j.scitotenv.2020.137647>, 2020.

575 Blackwell, B. D., & Driscoll, C. T.: Using foliar and forest floor mercury concentrations to assess spatial patterns of
576 mercury deposition. *Environmental Pollution*, 202, 126–134. <https://doi.org/10.1016/j.envpol.2015.02.036>,
577 2015.

578 Boening, D. W.: Ecological effects, transport, and fate of mercury: A general review. 17, 2000.

579 Borjac, J., El Joumaa, M., Kawach, R., Youssef, L., & Blake, D. A.: Heavy metals and organic compounds
580 contamination in leachates collected from Deir Kanoun Ras El Ain dump and its adjacent canal in South
581 Lebanon. *Heliyon*, 5(8), e02212. <https://doi.org/10.1016/j.heliyon.2019.e02212>, 2019.

582 Borjac, J., El Joumaa, M., Youssef, L., Kawach, R., & Blake, D. A.: Quantitative Analysis of Heavy Metals and
583 Organic Compounds in Soil from Deir Kanoun Ras El Ain Dump, Lebanon. *The Scientific World Journal*,
584 2020, 1–10. <https://doi.org/10.1155/2020/8151676>, 2020.

585 Briffa, J., Sinagra, E., & Blundell, R.: Heavy metal pollution in the environment and their toxicological effects on
586 humans. *Heliyon*, 6(9), e04691. <https://doi.org/10.1016/j.heliyon.2020.e04691>, 2020.

587 Carrasco-Gil, S., Estebarez-Yuberob, M., Medel-Cuestab, D., Millán, R., & Hernández, L. E.: Influence of nitrate
588 fertilization on Hg uptake and oxidative stress parameters in alfalfa plants cultivated in a Hg-polluted soil.
589 *Environmental and Experimental Botany*, 75. <https://doi.org/10.1016/j.envexpbot.2011.08.013>, 2012.

590 Cavallini, A., Natali, L., Durante, M., & Maserti, B. (1999). Mercury uptake, distribution and DNA affinity in
591 durum wheat (*Triticum durum* Desf.) plants. *Science of The Total Environment*, 243–244, 119–127.
592 [https://doi.org/10.1016/S0048-9697\(99\)00367-8](https://doi.org/10.1016/S0048-9697(99)00367-8).

593 Chen, X., Ji, H., Yang, W., Zhu, B., & Ding, H. Speciation and distribution of mercury in soils around gold mines
594 located upstream of Miyun Reservoir, Beijing, China. *Journal of Geochemical Exploration*, 163, 1–9.
595 <https://doi.org/10.1016/j.gexplo.2016.01.015>, 2016.

596 Clarkson, T. W., & Magos, L.: The Toxicology of Mercury and Its Chemical Compounds. *Critical Reviews in*
597 *Toxicology*, 36(8), 609–662. <https://doi.org/10.1080/10408440600845619>, 2006.

598 Dastoor, A., Angot, H., Bieser, J., Christensen, J. H., Douglas, T. A., Heimbürger-Boavida, L.-E., Jiskra, M., Mason,
599 R. P., McLagan, D. S., Obrist, D., Outridge, P. M., Petrova, M. V., Ryjkov, A., St. Pierre, K. A., Schartup,
600 A. T., Soerensen, A. L., Toyota, K., Travnikov, O., Wilson, S. J., & Zdanowicz, C.: Arctic mercury
601 cycling. *Nature Reviews Earth & Environment*, 3(4), Article 4. <https://doi.org/10.1038/s43017-022-00269->
602 [w](https://doi.org/10.1038/s43017-022-00269-w), 2022.

603 Demers, J. D., Blum, J. D., & Zak, D. R.: Mercury isotopes in a forested ecosystem: Implications for air-surface
604 exchange dynamics and the global mercury cycle: Mercury isotopes in a forested ecosystem. *Global*
605 *Biogeochemical Cycles*, 27(1), 222–238. <https://doi.org/10.1002/gbc.20021>, 2013.

606 Du, S.-H., & Fang, S. C.: Catalase activity of C3 and C4 species and its relationship to mercury vapor uptake.
607 *Environmental and Experimental Botany*, 23(4), 347–353. [https://doi.org/10.1016/0098-8472\(83\)90009-6](https://doi.org/10.1016/0098-8472(83)90009-6),
608 1983.

609 Duval, B., Gredilla, A., Fdez-Ortiz de Vallejuelo, S., Tessier, E., Amouroux, D., & de Diego, A.: A simple
610 determination of trace mercury concentrations in natural waters using dispersive Micro-Solid phase
611 extraction preconcentration based on functionalized graphene nanosheets. *Microchemical Journal*, 154,
612 104549. <https://doi.org/10.1016/j.microc.2019.104549>, 2020.

613 EJOLT: Cimenterie Nationale Factory in Chekaa, Lebanon | EJAtlas. *Environmental Justice Atlas*.
614 <https://ejatlas.org/conflict/chekaa>, Acces date: 2019.

615 Ericksen, J. A., Gustin, M. S., Schorran, D. E., Johnson, D. W., Lindberg, S. E., & Coleman, J. S.: Accumulation of
616 atmospheric mercury in forest foliage. *Atmospheric Environment*, 37(12), 1613–1622.
617 [https://doi.org/10.1016/S1352-2310\(03\)00008-6](https://doi.org/10.1016/S1352-2310(03)00008-6), 2003.

618 Ermolin, M. S., Fedotov, P. S., Malik, N. A., & Karandashev, V. K.: Nanoparticles of volcanic ash as a carrier for
619 toxic elements on the global scale. *Chemosphere*, 200, 16–22.
620 <https://doi.org/10.1016/j.chemosphere.2018.02.089>, 2018.

621 Freeman, M., & Carlson, R. M.: Essential nutrients. *Olive Production Manual*, 3353, 75, 2005.

622 Friedli, H. R., Arellano, A. F., Cinnirella, S., & Pirrone, N.: Initial Estimates of Mercury Emissions to the
623 Atmosphere from Global Biomass Burning. *Environmental Science & Technology*, 43(10), 3507–3513.
624 <https://doi.org/10.1021/es802703g>, 2009.

625 Galatali, S., A., N., & Kaya, E.: Characterization of Olive (*Olea Europaea* L.) Genetic Resources via PCR-Based
626 Molecular Marker Systems. 2, 26–33. <https://doi.org/10.24018/ejbio.2021.2.1.146>, 2021.

627 Gårdfeldt, K., Sommar, J., Ferrara, R., Ceccarini, C., Lanzillotta, E., Munthe, J., Wängberg, I., Lindqvist, O.,
628 Pirrone, N., Sprovieri, F., Pesenti, E., & Strömberg, D.: Evasion of mercury from coastal and open waters
629 of the Atlantic Ocean and the Mediterranean Sea. *Atmospheric Environment*, 37, 73–84.
630 [https://doi.org/10.1016/S1352-2310\(03\)00238-3](https://doi.org/10.1016/S1352-2310(03)00238-3), 2003.

631 Gérard, J., & Nehmé, C.: Lebanon. Méditerranée. *Revue Géographique Des Pays Méditerranéens / Journal of*
632 *Mediterranean Geography*, 131, Article 131. <https://journals.openedition.org/mediterranee/11018#>, 2020.

633 Giesler, R., Clemmensen, K. E., Wardle, D. A., Klaminder, J., & Bindler, R.: Boreal Forests Sequester Large
634 Amounts of Mercury over Millennial Time Scales in the Absence of Wildfire. *Environmental Science &*
635 *Technology*, 51(5), 2621–2627. <https://doi.org/10.1021/acs.est.6b06369>, 2017.

636 Grigal, D.: Mercury Sequestration in Forests and Peatlands: A Review. *Journal of Environmental Quality - J*
637 *ENVIRON QUAL*, 32. <https://doi.org/10.2134/jeq2003.0393>, 2003.

638 Guarino, F., Improta, G., Triassi, M., Castiglione, S., & Cicatelli, A.: Air quality biomonitoring through *Olea*
639 *europaea* L.: The study case of “Land of pyres.” *Chemosphere*, 282, 131052.
640 <https://doi.org/10.1016/j.chemosphere.2021.131052>, 2021.

641 Gworek, B., Dmuchowski, W., & Baczewska-Dąbrowska, A. H.: Mercury in the terrestrial environment: A review.
642 *Environmental Sciences Europe*, 32(1), 128. <https://doi.org/10.1186/s12302-020-00401-x>, 2020.

643 Hanson, P. J., Lindberg, S. E., Tabberer, T. A., Owens, J. G., & Kim, K.-H.: Foliar exchange of mercury vapor:
644 Evidence for a compensation point. *Water, Air, & Soil Pollution*, 80(1–4), 373–382.
645 <https://doi.org/10.1007/BF01189687>, 1995.

646 Higuera, P., Amorós, J. A., Esbrí, J. M., García-Navarro, F. J., Pérez de los Reyes, C., & Moreno, G.: Time and
647 space variations in mercury and other trace element contents in olive tree leaves from the Almadén Hg-
648 mining district. *Journal of Geochemical Exploration*, 123, 143–151.
649 <https://doi.org/10.1016/j.gexplo.2012.04.012>, 2012.

650 Higuera, P. L., Amorós, J. A., Esbrí, J. M., Pérez-de-los-Reyes, C., López-Berdonces, M. A., & García-Navarro, F.
651 J.: Mercury transfer from soil to olive trees. A comparison of three different contaminated sites.
652 *Environmental Science and Pollution Research*, 23(7), 6055–6061. [https://doi.org/10.1007/s11356-015-](https://doi.org/10.1007/s11356-015-4357-2)
653 [4357-2](https://doi.org/10.1007/s11356-015-4357-2), 2016.

654 Jindrich Petrik, Kodeih, N., IndyACT, Arnika Association, & IPEN WG.: Mercury in Fish and Hair Samples from
655 Batroun, Lebanon. <https://doi.org/10.13140/RG.2.2.12052.40327>, 2013.

656 Jiskra, M., Sonke, J. E., Obrist, D., Bieser, J., Ebinghaus, R., Myhre, C. L., Pfaffhuber, K. A., Wängberg, I.,
657 Kyllönen, K., Worthy, D., Martin, L. G., Labuschagne, C., Mkololo, T., Ramonet, M., Magand, O., &
658 Dommergue, A.: A vegetation control on seasonal variations in global atmospheric mercury concentrations.
659 *Nature Geoscience*, 11(4), 244–250. <https://doi.org/10.1038/s41561-018-0078-8>, 2018.

660 Johnson, & Lindberg: The biogeochemical cycling of Hg in forests: Alternative methods for quantifying total
661 deposition and soil emission. 1995, 80: 1069–1077, 9, 1995.

662 Jurdi, M., Korfali, S. I., Karahagopian, Y., & Davies, B. E.: Evaluation of Water Quality of the Qaraaoun Reservoir,
663 Lebanon: Suitability for Multipurpose Usage. 77(11–30), 20, 2002.

664 Kabata-Pendias, A., & Pendias, H.: Trace elements in soils and plants (3rd ed). CRC Press, 2000.

665 Khadari, B., El Bakkali, A., Essalouh, L., Tollon, C., Pinatel, C., & Besnard, G.: Cultivated Olive Diversification at
666 Local and Regional Scales: Evidence From the Genetic Characterization of French Genetic Resources.
667 *Frontiers in Plant Science*, 10. <https://www.frontiersin.org/articles/10.3389/fpls.2019.01593>, 2019.

668 Kobrossi, R., Nuwayhid, I., Sibai, A. M., El-Fadel, M., & Khogali, M.: Respiratory health effects of industrial air
669 pollution on children in North Lebanon. *International Journal of Environmental Health Research*, 12(3),
670 205–220. <https://doi.org/10.1080/09603/202/000000970>, 2002.

671 Kotnik, J., Sprovieri, F., Ogrinc, N., Horvat, M., & Pirrone, N.: Mercury in the Mediterranean, part I: Spatial and
672 temporal trends. *Environmental Science and Pollution Research*, 21(6), 4063–4080.
673 <https://doi.org/10.1007/s11356-013-2378-2>, 2014.

674 Labdaoui, D., Lotmani, B., & Aguedal, H.: Assessment of Metal Pollution on the Cultivation of Olive Trees in the
675 Petrochemical Industrial Zone of Arzew (Algeria). *South Asian Journal of Experimental Biology*, 11(3),
676 Article 3. [https://doi.org/10.38150/sajeb.11\(3\).p227-233](https://doi.org/10.38150/sajeb.11(3).p227-233), 2021.

677 Lebanon: Air Pollution | IAMAT: <https://www.iamat.org/country/lebanon/risk/air-pollution>, 2020

678 Li, D., Fang, K., Li, Y., Chen, D., Liu, X., Dong, Z., Zhou, F., Guo, G., Shi, F., Xu, C., & Li, Y.: Climate, intrinsic
679 water-use efficiency and tree growth over the past 150 years in humid subtropical China. *PLOS ONE*,
680 12(2), e0172045. <https://doi.org/10.1371/journal.pone.0172045>, 2017.

681 Li, R., Wu, H., Ding, J., Fu, W., Gan, L., & Li, Y.: Mercury pollution in vegetables, grains and soils from areas
682 surrounding coal-fired power plants. *Scientific Reports*, 7(1), 46545. <https://doi.org/10.1038/srep46545>,
683 2017.

684 Lindberg, S., Bullock, R., Ebinghaus, R., Engstrom, D., Feng, X., Fitzgerald, W., Pirrone, N., Prestbo, E., &
685 Seigneur, C.: A Synthesis of Progress and Uncertainties in Attributing the Sources of Mercury in
686 Deposition. *Ambio*, 36(1), 19–32, 2007.

687 Lindberg, S. E., Jackson, D. R., Huckabee, J. W., Janzen, S. A., Levin, M. J., & Lund, J. R.: Atmospheric Emission
688 and Plant Uptake of Mercury from Agricultural Soils near the Almadén Mercury Mine. *Journal of*
689 *Environmental Quality*, 8(4), 572–578. <https://doi.org/10.2134/jeq1979.00472425000800040026x>, 1979

690 Lodenius, M., Tulisalo, E., & Soltanpour-Gargari, A.: Exchange of mercury between atmosphere and vegetation
691 under contaminated conditions. *Science of The Total Environment*, 304(1–3), 169–174.
692 [https://doi.org/10.1016/S0048-9697\(02\)00566-1](https://doi.org/10.1016/S0048-9697(02)00566-1), 2003.

693 Luo, Y., Duan, L., Driscoll, C. T., Xu, G., Shao, M., Taylor, M., Wang, S., & Hao, J.: Foliage/atmosphere exchange
694 of mercury in a subtropical coniferous forest in south China. *Journal of Geophysical Research:*
695 *Biogeosciences*, 121(7), 2006–2016. <https://doi.org/10.1002/2016JG003388>, 2016.

696 Maillard, F., Girardclos, O., Assad, M., Zappellini, C., Pérez Mena, J. M., Yung, L., Guyeux, C., Chrétien, S.,
697 Bigham, G., Cosio, C., & Chalot, M.: Dendrochemical assessment of mercury releases from a pond and
698 dredged-sediment landfill impacted by a chlor-alkali plant. *Environmental Research*, 148, 122–126.
699 <https://doi.org/10.1016/j.envres.2016.03.034>, 2016.

700 McLagan, D. S., Biester, H., Navrátil, T., Kraemer, S. M., & Schwab, L.: Internal tree cycling and atmospheric
701 archiving of mercury: Examination with concentration and stable isotope analyses. *Biogeosciences*, 19, 4415–4429,
702 2022. <https://doi.org/10.5194/bg-19-4415-2022>, 2022.

703 McLagan, D. S., Stupple, G. W., Darlington, A., Hayden, K., Steffen, A., & Kamp, L.: Where there is smoke there is
704 mercury: Assessing boreal forest fire mercury emissions using aircraft and highlighting uncertainties
705 associated with upscaling emissions estimates. *Atmos. Chem. Phys.*, 19, 2021.

706 Naharro, R., Esbri, J., Amorós, J., & Higuera, P.: Atmospheric mercury uptake and desorption from olive-tree
707 leaves. *20(EGU2018-2982,2018)*, 2, 2018

708 Nassif, N., Jaoude, L. A., El Hage, M., & Robinson, C. A.: Data Exploration and Reconnaissance to Identify Ocean
709 Phenomena: A Guide for <i>In Situ</i> Data Collection. *Journal of Water Resource and*
710 *Protection*, 08(10), 929–943. <https://doi.org/10.4236/jwarp.2016.810076>, 2016.

711 Niu, Z., Zhang, X., Wang, Z., & Ci, Z.: Field controlled experiments of mercury accumulation in crops from air and
712 soil. *Environmental Pollution*, 159(10), 2684–2689. <https://doi.org/10.1016/j.envpol.2011.05.029>

713 Obrist, D.: Atmospheric mercury pollution due to losses of terrestrial carbon pools? *Biogeochemistry*, 85(2), 119–
714 123. <https://doi.org/10.1007/s10533-007-9108-0>, 2011, 2007

715 Obrist, D., Johnson, D. W., & Lindberg, S. E.: Mercury concentrations and pools in four Sierra Nevada forest sites,
716 and relationships to organic carbon and nitrogen. 13, 2009.

717 Obrist, D., Kirk, J. L., Zhang, L., Sunderland, E. M., Jiskra, M., & Selin, N. E.: A review of global environmental
718 mercury processes in response to human and natural perturbations: Changes of emissions, climate, and land
719 use. *Ambio*, 47(2), 116–140. <https://doi.org/10.1007/s13280-017-1004-9>, 2018.

720 Obrist, M. K., Rathey, E., Bontadina, F., Martinoli, A., Conedera, M., Christe, P., & Moretti, M.: Response of bat
721 species to sylvo-pastoral abandonment. *Forest Ecology and Management*, 261(3), 789–798.
722 <https://doi.org/10.1016/j.foreco.2010.12.010>, 2011.

723 O’Connor, D., Hou, D., Ok, Y. S., Mulder, J., Duan, L., Wu, Q., Wang, S., Tack, F. M. G., & Rinklebe, J.: Mercury
724 speciation, transformation, and transportation in soils, atmospheric flux, and implications for risk
725 management: A critical review. *Environment International*, 126, 747–761.
726 <https://doi.org/10.1016/j.envint.2019.03.019>, 2019.

727 Ozturk, M., Altay, V., Gönenç, T. M., Unal, B. T., Efe, R., Akçiçek, E., & Bukhari, A.: An Overview of Olive
728 Cultivation in Turkey: Botanical Features, Eco-Physiology and Phytochemical Aspects. *Agronomy*, 11(2),
729 295. <https://doi.org/10.3390/agronomy11020295>, 2021.

730 Patra, M., & Sharma, A.: Mercury toxicity in plants. *The Botanical Review*, 66(3), 379–422.
731 <https://doi.org/10.1007/BF02868923>, 2000

732 Pleijel, H., Klingberg, J., Nerentorp, M., Broberg, M. C., Nyirambangutse, B., Munthe, J., & Wallin, G.: Mercury
733 accumulation in leaves of different plant types – the significance of tissue age and specific leaf area. *Biogeosciences*,
734 18, 6313–6328, 2021. <https://doi.org/10.5194/bg-18-6313-2021>, 2021.

735 Pokharel, A. K., & Obrist, D.: Fate of mercury in tree litter during decomposition. *Biogeosciences*, 8(9), 2507–2521.
736 <https://doi.org/10.5194/bg-8-2507-2011>, 2011.

737 Rea, A. W., Keeler, G. J., & Scherbatskoy, T.: The deposition of mercury in throughfall and litterfall in the lake
738 champlain watershed: A short-term study. *Atmospheric Environment*, 30(19), 3257–3263.
739 [https://doi.org/10.1016/1352-2310\(96\)00087-8](https://doi.org/10.1016/1352-2310(96)00087-8), 1996.

740 Rea, A. W., Lindberg, S. E., Scherbatskoy, T., & Keeler, G. J.: Mercury Accumulation in Foliage over Time in Two
741 Northern Mixed-Hardwood Forests. 19, 2002

742 Richardson, J. B., Friedland, A. J., Engerbretson, T. R., Kaste, J. M., & Jackson, B. P.: Spatial and vertical
743 distribution of mercury in upland forest soils across the northeastern United States. *Environmental*
744 *Pollution (Barking, Essex : 1987)*, 182, 127–134. <https://doi.org/10.1016/j.envpol.2013.07.011>, 2013.

745 Sanz-Cortés, F., Martínez-Calvo, J., Badenes, M. L., Bleiholder, H., Hack, H., Llacer, G., & Meier, U.: Phenological
746 growth stages of olive trees (*Olea europaea*). *Annals of Applied Biology*, 140(2), 151–157.
747 <https://doi.org/10.1111/j.1744-7348.2002.tb00167.x>, 2002.

748 Schaefer, K., Elshorbany, Y., Jafarov, E., Schuster, P. F., Striegl, R. G., Wickland, K. P., & Sunderland, E. M.:
749 Potential impacts of mercury released from thawing permafrost. *Nature Communications*, 11(1), Article 1.
750 <https://doi.org/10.1038/s41467-020-18398-5>, 2020.

751 Schneider, L., Allen, K., Walker, M., Morgan, C., & Haberle, S.: Using Tree Rings to Track Atmospheric Mercury
752 Pollution in Australia: The Legacy of Mining in Tasmania. *Environmental Science & Technology*, 53(10),
753 5697–5706. <https://doi.org/10.1021/acs.est.8b06712>, 2019.

754 Schwesig, D., & Krebs, O.: The role of ground vegetation in the uptake of mercury and methylmercury in a forest
755 ecosystem. *Plant and Soil*, 11, 2003.

756 Senesil, G. S., Baldassarre, G., Senesi, N., & Radina, B.: Trace element inputs into soils by anthropogenic activities
757 and implications for human health. *Chemosphere*, 39(2), 343–377. [https://doi.org/10.1016/S0045-](https://doi.org/10.1016/S0045-6535(99)00115-0)
758 [6535\(99\)00115-0](https://doi.org/10.1016/S0045-6535(99)00115-0), 1999.

759 Sghaier, A., Perttunen, J., Sievaänen, R., Boujnah, D., Ouessar, M., Ben Ayed, R., & Naggaz, K.: Photosynthetical
760 activity modelisation of olive trees growing under drought conditions. *Scientific Reports*, 9(1), 15536.
761 <https://doi.org/10.1038/s41598-019-52094-9>, 2019.

762 Teixeira, D. C., Lacerda, L. D., & Silva-Filho, E. V.: Mercury sequestration by rainforests: The influence of
763 microclimate and different successional stages. *Chemosphere*, 168, 1186–1193.
764 <https://doi.org/10.1016/j.chemosphere.2016.10.081>, 2017.

765 Terral, J.-F., Alonso, N., Capdevila, R. B. i, Chatti, N., Fabre, L., Fiorentino, G., Marinval, P., Jordá, G. P., Pradat,
766 B., Rovira, N., & Alibert, P.: Historical biogeography of olive domestication (*Olea europaea* L.) as revealed
767 by geometrical morphometry applied to biological and archaeological material: Historical biogeography of
768 olive domestication (*Olea europaea* L.). *Journal of Biogeography*, 31(1), 63–77.
769 <https://doi.org/10.1046/j.0305-0270.2003.01019.x>, 2004

770 Tomiyasu, T., Matsuo, T., Miyamoto, J., Imura, R., Anazawa, K., & Sakamoto, H.: Low level mercury uptake by
771 plants from natural environments—Mercury distribution in *Solidago altissima* L.-. *Environmental Sciences:*
772 *An International Journal of Environmental Physiology and Toxicology*, 12(4), 231–238, 2005.

773 UNEP: Technical Background Report to the Global Mercury Assessment 2018. IVL Svenska Miljöinstitutet, 2019.

774 Wang, X., Lin, C.-J., Lu, Z., Zhang, H., Zhang, Y., & Feng, X.: Enhanced accumulation and storage of mercury on
775 subtropical evergreen forest floor: Implications on mercury budget in global forest ecosystems: Hg storage
776 on subtropical forest floor. *Journal of Geophysical Research: Biogeosciences*, 121(8), 2096–2109.
777 <https://doi.org/10.1002/2016JG003446>, 2016.

778 Wofsy, S. C., Goulden, M. L., Munger, J. W., Fan, S.-M., Bakwin, P. S., Daube, B. C., Bassow, S. L., & Bazzaz, F.
779 A.: Net Exchange of CO₂ in a Mid-Latitude Forest. *Science*, 260(5112), 1314–1317.
780 <https://doi.org/10.1126/science.260.5112.1314>, 1993.

781 Wohlgemuth, L., Rautio, P., Ahrends, B., Russ, A., Vesterdal, L., Waldner, P., Timmermann, V., Eickenscheidt, N.,
782 Fürst, A., Greve, M., Roskams, P., Thimonier, A., Nicolas, M., Kowalska, A., Ingerslev, M., Merilä, P.,
783 Benham, S., Iacoban, C., Hoch, G., ... Jiskra, M.: Physiological and climate controls on foliar mercury
784 uptake by European tree species. *Biogeosciences*, 19, 1335–1353, 2022. [https://doi.org/10.5194/bg-19-](https://doi.org/10.5194/bg-19-1335-2022)
785 [1335-2022](https://doi.org/10.5194/bg-19-1335-2022), 2021.

786 Wright, L. P., Zhang, L., & Marsik, F. J.: Overview of mercury dry deposition, litterfall, and throughfall studies.
787 *Atmospheric Chemistry and Physics*, 16(21), 13399–13416. <https://doi.org/10.5194/acp-16-13399-2016>,
788 2016.

789 Yammine, P., Kfoury, A., El-Khoury, B., Nouali, H., El-Nakat, H., Ledoux, F., Courcot, D., & Aboukaïs, A.: A
790 preliminary evaluation of the inorganic chemical composition of atmospheric tsp in the selaata region,
791 north lebanon. *Lebanese Science Journal*, 11(1), 18, 2010.

792 Yanai, R. D., Yang, Y., Wild, A. D., Smith, K. T., & Driscoll, C. T.: New Approaches to Understand Mercury in
793 Trees: Radial and Longitudinal Patterns of Mercury in Tree Rings and Genetic Control of Mercury in
794 Maple Sap. *Water, Air, & Soil Pollution*, 231(5), 248. <https://doi.org/10.1007/s11270-020-04601-2>, 2020

795 Yang, Y., Yanai, R. D., Driscoll, C. T., Montesdeoca, M., & Smith, K. T.: Concentrations and content of mercury in
796 bark, wood, and leaves in hardwoods and conifers in four forested sites in the northeastern USA. *PLOS*
797 *ONE*, 13(4), e0196293. <https://doi.org/10.1371/journal.pone.0196293>, 2018.

798 Yazbeck, E. B., Rizk, G. A., Hassoun, G., El-Khoury, R., & Geagea, L.: Ecological characterization of ancient olive
799 trees in Lebanon- Bshaaleh area and their age estimation. 11(2 Ver. 1), 35–44, 2018.

800 Zhao, X., & Wang, D.: Mercury in some chemical fertilizers and the effect of calcium superphosphate on mercury
801 uptake by corn seedlings (*Zea mays* L.). *Journal of Environmental Sciences*, 22(8), 1184–1188.
802 [https://doi.org/10.1016/S1001-0742\(09\)60236-9](https://doi.org/10.1016/S1001-0742(09)60236-9), 2010

803 Zhou, J., Obrist, D., Dastoor, A., Jiskra, M., & Ryjkov, A.: Vegetation uptake of mercury and impacts on global
804 cycling. *Nature Reviews Earth & Environment*, 2(4), 269–284. [https://doi.org/10.1038/s43017-021-00146-](https://doi.org/10.1038/s43017-021-00146-y)
805 [y](https://doi.org/10.1038/s43017-021-00146-y), 2021

806 Zhou, J., Wang, Z., & Zhang, X.: Deposition and Fate of Mercury in Litterfall, Litter, and Soil in Coniferous and
807 Broad-Leaved Forests. *Journal of Geophysical Research: Biogeosciences*, 123(8), 2590–2603.
808 <https://doi.org/10.1029/2018JG004415>, 2018.